Electron Distribution and Bonding in η^3-Cyclopropenyl–Metal Complexes

Dennis L. Lichtenberger,* Martin L. Hoppe, Lalitha Subramanian, and Edward M. Kober

Laboratory for Electron Spectroscopy and Surface Analysis, Department of Chemistry, University of Arizona, Tucson, Arizona 85721

Russell P. Hughes, John L. Hubbard,† and David S. Tucker

Department of Chemistry, Burke Laboratory, Dartmouth College, Hanover, New Hampshire 03755

Received September 29, 1992

The synthesis of $(\eta^3\text{-}C_3R_3)Ir(CO)_3$ and He I and He II photoelectron spectra of $(\eta^3\text{-}C_3R_3)Co(CO)_3$, $(\eta^3\text{-}C_3R_3)Ir(CO)_3$, and $(\eta^3\text{-}C_3R_3)Fe(CO)_2(NO)$ (where R = *tert*-butyl) are reported. The shifts and splittings in ionization energies with the metal and ligand perturbations in this series, the changes in ionization peak areas as a function of the excitation energy, and Fenske–Hall molecular orbital calculations assist in the assignment and interpretation of the spectra. The cobalt complex reveals three peaks in the low ionization energy region that are primarily metal-based, consistent with the two states of e symmetry and one state of a_1 symmetry from the five d orbitals of a formally d^{10} metal in C_{3v} symmetry. The spectrum of the iridium complex has five peaks in this region due to large spin-orbit coupling that splits the e symmetry ionizations. The doubly degenerate peaks of the cobalt complex are also expected to be split in the photoelectron spectrum of the iron-nitrosyl complex due to the lowering to C_s symmetry. Only four distinct peaks are seen for the iron–nitrosyl complex, with two ionization bands at higher energy being merged in a broad envelope. The ionization cross-sections indicate that the η^3-bound C_3R_3 ligand in these complexes is best described formally as a cation with a large amount of mixing and backbonding from the metal d_π orbitals to the e_{π^*} orbitals of the cyclopropenyl ring. This is compared to the NO^+ ligand.

Introduction

Metallacyclobutadienes **1** and η^3-cyclopropenyl metal complexes **2** are both possible intermediates in alkyne metathesis reactions.[1] One mechanism of metathesis involves formation of a metallacyclobutadiene intermediate generated via parallel attack of the free alkyne with respect to the M–C triple bond. The other mechanism

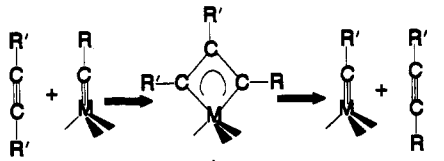

1

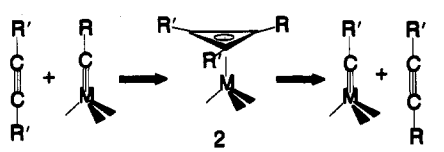

2

involves formation of an η^3-cyclopropenyl intermediate generated via perpendicular attack of the free alkyne across the M–C triple bond. Structures **1** and **2** can also result from a reaction between metal complex and a cyclopropenyl cation. An elaborate theoretical study of the bonding interactions of ML_5, ML_4, ML_3, and ML_2 complexes with the cyclopropenyl ring has been presented.[2] A thorough analysis of different ML_n (where L = CO) fragments show that while ML_5 prefers an η^1 cyclopropenyl coordination, ML_4 and ML_2 are similar and prefer an η^2 ring coordination which could easily lead to a metallacyclobutadiene geometry. On the other hand, ML_3 systems prefer an η^3 ring coordination. There exists a substantial amount of experimental, primarily crystallographic, data on complexes where the cyclopropenyl ring is bound in an η^1, η^2, or η^3 fashion.[3–10]

The present work is mainly concerned with the electronic structure of η^3-cyclopropenyl metal complexes. This paper presents the results of He I and He II UV–photoelectron spectroscopic studies on $(\eta^3\text{-}C_3R_3)Co(CO)_3$, **I**, $(\eta^3\text{-}C_3R_3)Ir(CO)_3$ **II**, and the isoelectronic $(\eta^3\text{-}C_3R_3)Fe(CO)_2(NO)$ **III** (where *R* = *tert*-butyl). The frontier orbitals of primary interest derive from the π symmetry orbitals of the cyclopropenyl ring and the d orbitals of the metal. The π symmetry orbitals of the cyclopropenyl ring will be referred to as the a_π and the e_{π^*} orbitals. Because the e_{π^*} orbitals are net antibonding in the ring, it is natural to

* Author to whom correspondence should be addressed.
† Current address: Department of Chemistry and Biochemistry, Utah State University, Logan, Utah 84322.

(1) Schrock, R. R. *Acc. Chem. Res.* **1986**, *19*, 342.
(2) Jemmis, E. D.; Hoffmann, R. *J. Am. Chem. Soc.* **1980**, *102*, 2570.
(3) Gompper, R.; Bartmann, E.; Nöth, H. *Chem. Ber.* **1979**, *112*, 218.
(4) DeSimone, D. M.; Desrosiers, P. J.; Hughes, R. P. *J. Am. Chem. Soc.* **1982**, *104*, 4842.
(5) Desrosiers, P. J.; Hughes, R. P. *J. Am. Chem. Soc.* **1981**, *103*, 5593.
(6) McClure, M. D.; Weaver, D. L. *J. Organomet. Chem.* **1973**, *54*, C59.
(7) Hughes, R. P.; Lambert, J. M. J.; Whitman, D. W.; Hubbard, J. L.; Henry, W. P.; Rheingold, A. L. *Organometallics* **1986**, *5*, 789.
(8) Gowling, E. W.; Kettle, S. F. A. *Inorg. Chem.* **1964**, *3*, 604.
(9) Rausch, M. D.; Tuggle, R. M.; Weaver, D. L. *J. Am. Chem. Soc.* **1970**, *92*, 4981.
(10) (a) Tuggle, R. M.; Weaver, D. L. *Inorg. Chem.* **1971**, *10*, 1504; (b) **1971**, *10*, 2599.

0276-7333/93/2312-2025$04.00/0

begin the formal description in terms of a $C_3R_3^+$ cation with empty e_{π^*} orbitals. The metals in these complexes then have formal d^{10} configuration. Although this is only a formal starting point for describing these complexes, the essence of this description is supported by the photoelectron spectroscopic information reported in this paper. More detailed information is provided on the nature of the highest occupied molecular orbital (HOMO), the nature of the bonding between the ring and the metal carbonyl fragment, and the strength of interaction between the cyclopropenyl ring and the metal center.

It is also informative to compare these results with other isoelectronic complexes. The cyclopropenyl cobalt complex **I** (compound **3**) studied here is the final member of a series of cobalt metallatetrahedranes $[Co_2(CO)_6C_2R_2]$[11] **4**, $[Co_3(CO)_9CR)]$[12] **5**, and $[Co_4(CO)_{12}]$[13] **6** (the three carbonyl ligands on each cobalt are not shown in the structures for clarity). The cyclopropenyl cation ligand

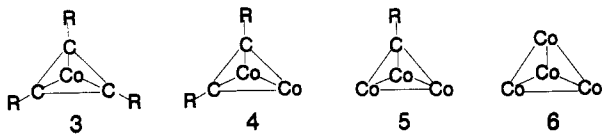

is also isolobal[14,15] with NO^+. Some photoelectron spectroscopic studies on related complexes have been published which include $[Co(CO)_3(NO)]$[16] and $[Fe(CO)_2(NO)_2]$.[16] This comparison will emphasize the similarities and differences between the cyclopropenyl and nitrosyl ligands.

Experimental Section

The title compounds were prepared by published procedures,[7] except for the new compound $(\eta^3\text{-}C_3R_3)Ir(CO)_3$ which was prepared as detailed below. All manipulations with the compounds were carried out in a dry N_2-filled Vacuum Atmospheres glovebox.

Photoelectron Spectra. He I and He II gas-phase photoelectron spectra were recorded using an McPherson ESCA36 instrument that features a 36-cm hemispherical analyzer (10-cm gap). Data collection methods are described elsewhere.[17,18] The spectra were measured with the sample ionization cell at approximately 35 ± 3 °C for the Co and Fe complexes and at 50 ± 3 °C for the Ir complex. The argon $^2P_{3/2}$ ionization at 15.759 eV was used as an internal calibration lock of the energy scale. During collection the instrument resolution was better than 25 meV. He II (40.81 eV) spectra were corrected for ionizations from He II β source excitation which is at 7.214 eV lower binding energy and has 12% of the intensity of He II α line. The data was intensity corrected for the experimentally determined analyzer sensitivity versus electron kinetic energy. The ionizations were modeled analytically with asymmetric Gaussian peaks. The program is a modification of a previously published[19] one with the incorporation of constraints and boundary conditions used in the programs of Lichtenberger et al.[20,21] Each band is defined by the peak position, amplitude, half-width on the high binding energy side of the peak, and the half-width on the low binding energy side of the peak. The error in peak positions and half-widths is within ±0.02 eV (≈3σ level). Based solely on the features of a given band profile, a minimum number of peaks were used to fit the experimental data. The parameters describing an individual ionization peak are less certain (±0.04 eV) when two or more peaks are close in energy and overlapping. The confidence limits for the relative integrated peak areas are about 5%, with the primary source of uncertainty being the determination of the base line subtracted from the peak. More detailed discussion of modeling criteria are described in the literature.[21] For representation of the He II data, the position and width values of the asymmetric Gaussians were all constrained to He I values, which were more accurately determined from the He I spectra. The amplitudes were then allowed to vary to account for the different cross-sections for the He II ionizations.

General Procedures. All reactions were performed under a dinitrogen atmosphere using standard Schlenk techniques. The dinitrogen was deoxygenated over BASF catalyst and dried over Aquasorb. IR spectra were obtained on a Bio-Rad FTS 40 spectrometer. The ^1H (300 MHz) and $^{13}C\{^1H\}$ (75 MHz) NMR spectra were obtained on a Varian Associates XL-300 spectrometer at 22 °C. All solvents were dinitrogen saturated. Methylene chloride and hexanes were distilled over calcium hydride. (Bis(triphenylphosphine)nitrogen(1+))tetracarbonyliridate, PPN[Ir(CO)$_4$],[22] and tri-*tert*-butylcyclopropenyl tetrafluoroborate, $[C_3{}^tBu_3][BF_4]$,[23] were prepared by literature procedures.

Synthesis of $(\eta^3\text{-}C_3{}^tBu_3)Ir(CO)_3$ (II). A solution of $[C_3{}^tBu_3][BF_4]$ (0.745 g, 2.52 mmol) in CH_2Cl_2 (20 mL) was dripped into an orange solution of thoroughly dried PPN[Ir(CO)$_4$] (2.12 g, 2.52 mmol) in CH_2Cl_2 (10 mL). After 5 min, the addition was complete and the color changed to deep red. After 2 h of stirring, the volatiles were removed in vacuo affording a red solid. Extraction from hexanes (3 × 15 mL) followed by solvent removal afforded the air-stable white solid **II** (0.978 g, 2.02 mmol, 80%). If additional purification is desired, **II** may be filtered through an alumina column (1 in. × 1 in.) in air. This complex may be sublimed (0.01 Torr, 80 °C) or recrystallized from hexanes to afford white cubes: mp 158 °C dec; IR (hexanes) ν(CO) = 2056, 1993 cm^{-1}; ^1H NMR ($CDCl_3$) δ 1.23 (s); $^{13}C\{^1H\}$ NMR ($CDCl_3$) δ 171.06 (*C*O), 46.93 (*C*^{t}Bu), 31.65 (*C*H$_3$), 27.79 (*C*Me$_3$). Anal. Calcd for $C_{18}H_{27}IrO_3$: C, 44.70; H, 5.63; Found: C, 44.67; H, 5.64.

Fenske–Hall Calculations. Orbital eigenvalues were calculated by the Fenske–Hall method[24] for the systems $(\eta^3\text{-}C_3H_3)Co(CO)_3$ and $(\eta^3\text{-}C_3H_3)Fe(CO)_2(NO)$. The symmetry of the cyclopropenyl complexes was idealized to C_{3v}. The bond angles and distances were based on the structure of a related cyclopropenyl complex, $(CPh)_3Co(CO)_3$, determined by single-crystal X-ray diffraction experiments.[25] The Co–C(CO) distance was set at 1.80 Å, Co–C(ring) at 2.01 Å, C–C(ring) at 1.42 Å, and C–O at 1.13 Å. The angle subtended by the carbonyl and the centroid of the ring at the metal was 109° in accordance with the crystal structure. The bond distance for Fe–N was set at 1.74 Å and that for N–O was set at 1.15 Å based on the structure of the analogous compound, $(Ph_2{}^tBuC_3)Fe(CO)_2(NO)$. Atomic basis functions for Co and Fe were generated from Herman–Skillman atomic calculations using Herski and Basis according to the method of Bursten, Fenske, and Jensen.[26]

(11) van Dam, H.; Stufkens, D. J.; Oskam, A.; Doran, M.; Hillier, I. H. *J. Electr. Spectry. Relat. Phenom.* **1980**, *21*, 47.
(12) Chesky, P. T.; Hall, M. B. *Inorg. Chem.* **1981**, *20*, 4419.
(13) Dekock, R. L.; Wong, K. S.; Fehlner, T. P. *Inorg. Chem.* **1982**, *21*, 3203.
(14) Elian, M.; Chen, M. M. L.; Mingos, D. M. P.; Hoffmann, R. *Inorg. Chem.* **1976**, *15*, 1148.
(15) Hoffmann, R. *Angew. Chem.* **1982**, *94*, 725; *Angew. Chem. Int. Ed.* **1982**, *21*, 711.
(16) Hillier, I. H.; Guest, M. F.; Higginson, B. R.; Lloyd, D. R. *Mol. Phys.* **1974**, *27*, 215.
(17) Kellogg, G. E. *Diss. Abstr. Intl.* **1986**, *46*, 3838.
(18) Jatcko, M. E. *Diss. Abstr. Intl. B* **1990**, *51(1)*, 200.
(19) Chandramouli, G. V. R.; Lalitha, S.; Manoharan, P. T. *Comput. Chem.* **1990**, *14*, 257.
(20) Lichtenberger, D. L.; Fenske, R. F. *J. Am. Chem. Soc.* **1976**, *98*, 50.
(21) Lichtenberger, D. L.; Copenhaver, A. S. *J. Electron Spectry. Relat. Phenom.* **1990**, *50*, 335.
(22) Garlaschelli, L.; Della Pergola, R. *Inorg. Synth.* **1991**, *28*, 211.
(23) Ciabattoni, J.; Nathan, E. C.; Feiring, A. E.; Kocienski, P. J. *Org. Synth.* **1974**, *54*, 97.
(24) Hall, M. B.; Fenske, R. F. *Inorg. Chem.* **1972**, *11*, 768.
(25) Chiang, T.; Kerber, R. C.; Kimball, S. D.; Lauher, J. W. *Inorg. Chem.* **1979**, *18*, 1687.
(26) Bursten, B. E.; Jensen, J. R.; Fenske, R. F. *J. Chem. Phys.* **1978**, *68*, 3320.

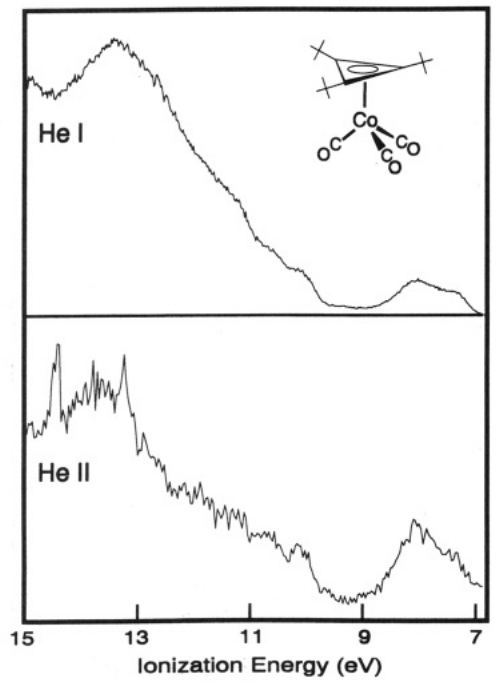

Figure 1. He I and He II photoelectron spectra for (η^3-C_3R_3)$Co(CO)_3$ (where R = *tert*-butyl).

Photoelectron Spectra and Ionization Band Assignments

(η^3-C_3R_3)$Co(CO)_3$. He I and He II photoelectron spectra of (η^3-C_3R_3)$Co(CO)_3$ (where R = *tert*-butyl) are shown in Figure 1 for the full valence region from 7.0 to 15.0 eV. The region above 10.0 eV is primarily ligand-based ionizations and includes multiple overlapping ionizations of C–C and C–H σ bonds. Individual assignments in this region will not be attempted. The most useful information in this region is the shoulders located between 10.0 and 11.0 eV, which can be used for comparisons of ionization intensities. The primary benefit of obtaining both He I and He II data is that the relative amount of metal or ligand character of a particular ionization band can be determined since it has been shown both experimentally[27,28] and theoretically[29] that the photoionization cross-sections are different for different orbitals. From atomic calculations,[29] the photoionization cross-section for carbon 2p electrons decreases from 6.1 in He I to 1.9 in He II while for cobalt 3d it increases from 4.8 in He I to 8.7 in He II. For oxygen 2p the cross-section decreases from 10.6 in He I to 6.8 in He II.[29] The ionizations in the region between 7.0 and 9.0 eV show an increase in relative intensity when He II source radiation is used. The shoulders located between 10.0 and 11.0 eV show a decrease in relative intensity when the source is changed from He I to He II. This indicates that the metal-based ionizations are in the region below 9.0 eV. The following discussion will be restricted to the analysis of the metal-based ionizations between 7.0 and 9.0 eV. Figure 2 shows He I and He II photoelectron spectra of this region for (η^3-C_3R_3)$Co(CO)_3$. Numbers shown in the He II spectrum correspond to the change in the relative band intensity (relative to band C) compared to the He I spectrum.

Before going into the details of the 7–9 eV region, it is instructive to look at the molecular orbital diagram

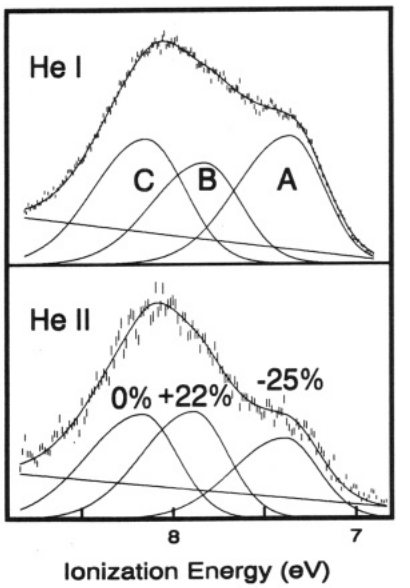

Figure 2. He I and He II photoelectron spectra of (η^3-C_3R_3)$Co(CO)_3$ (where R = *tert*-butyl) in the region 8.9–6.9 eV. Numbers shown in the He II spectrum correspond to the change in the relative band intensity (relative to band C) compared to the He I spectrum.

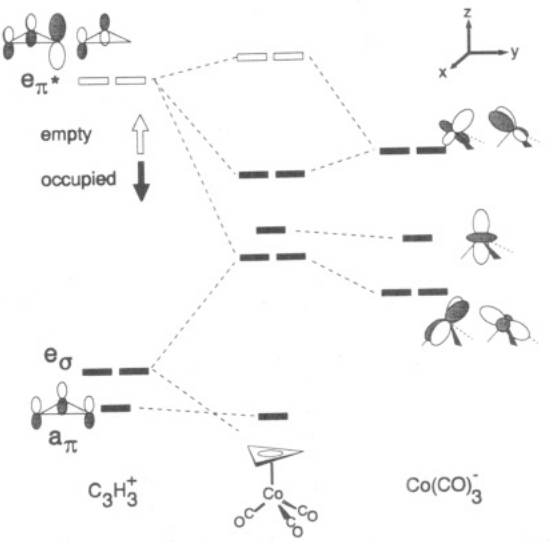

Figure 3. Molecular orbital diagram for (η^3-C_3H_3)$Co(CO)_3$ based on Fenske–Hall calculations.

generated by Fenske–Hall calculations (Figure 3). The three-legged piano-stool molecule can be built from $C_3H_3^+$ and $Co(CO)_3^-$ fragments, where Co has a formal oxidation state of –1 resulting in a d^{10} configuration. Theoretically, this molecule can also be constructed from neutral fragments of C_3H_3 and $Co(CO)_3$. The π orbitals of the cyclopropenyl fragment give rise to a_{π} below e_{π^*} pattern. Just above the occupied a_{π} level, the Fenske–Hall calculation places a degenerate e_{σ} level. The orbitals of the $Co(CO)_3^-$ fragment give rise to e below a below e pattern which is expected for the ML_3 (C_{3v}) unit.[30] The HOMO is primarily the d_{xz}, d_{yz} orbital set of e symmetry which interacts with the cyclopropenyl e_{π^*} orbital. The calculations predict the HOMO to be made up of 40% metal d and 25% cyclopropenyl e_{π^*}. The calculated energy separation between the HOMO and the second highest occupied molecular orbital is approximately 1 eV. The

(27) Lichtenberger, D. L.; Calabro, D. C.; Kellogg, G. E. *Organometallics* **1984**, *3*, 1623.
(28) Lichtenberger, D. L.; Kellogg, G. E. *Acc. Chem. Res.* **1987**, *20*, 379.
(29) Yeh, J. J.; Lindau, I. *Atom. Nucl. Data. Tabs.* **1985**, *32*, 7.
(30) Albright, T. A.; Burdett, J. K.; Whangbo, M. H. *Orbital Interactions in Chemistry*; John Wiley & Sons: New York, 1985.

Table I. He I and He II Ionization Data

peak	position (eV)	relative area He I	relative area He II	width high	width low
		$(\eta^3\text{-}C_3R_3)Co(CO)_3$			
A	7.36	0.96	0.73	0.68	0.43
B	7.85	0.79	0.97	0.67	0.47
C	8.15	1.00	1.00	0.67	0.50
		$(\eta^3\text{-}C_3R_3)Ir(CO)_3$			
A1	7.53	0.95	0.55	0.52	0.36
A2	8.01	0.69	0.47	0.48	0.29
B	8.55	0.69	0.82	0.55	0.37
C1	9.02	0.47	0.41	0.24	0.24
C2	9.30	1.00	1.00	0.55	0.31
		$(\eta^3\text{-}C_3R_3)Fe(CO)_2(NO)$			
A1	7.19	0.48	0.23	0.43	0.37
A2	7.53	0.51	0.35	0.40	0.40
C1	7.81	0.45	0.41	0.41	0.41
B, C2	8.28	1.00	1.00	0.66	0.43

second filled orbital is of a_1 symmetry and has 70% d_{z^2} orbital character. It is destabilized slightly by a filled–filled interaction with the a_π orbital of the ring. Below this level is the other e set with approximately 45% metal d character composed mainly of $d_{x^2-y^2}$ and d_{xy} orbitals.

The HOMO, having the primary bonding interaction between the ring and the metal center, constitutes band A in the Co spectrum shown in Figure 2. Band B corresponds primarily to the a_1 symmetry Co d_{z^2}. Band C is assigned to the metal $d_{x^2-y^2}$ and d_{xy} orbitals stabilized by strong back-bonding to the CO π^* orbitals. Evidence consistent with this assignment is seen from the comparison of the peak areas between He I and He II data shown in Table I. The percentage change in relative intensity of each of the bands with respect to band C is shown in Figure 2. There is substantial loss in intensity of band A relative to band B and C indicating substantial carbon character in band A. The relative increase in band B in the He II spectra indicates that band B has a substantial amount of metal d character and therefore supports the assignment of band B as primarily the d_{z^2} orbital on the metal atom. The experiment does indicate more delocalization than the calculation.

$(\eta^3\text{-}C_3R_3)Ir(CO)_3$. Figure 4 shows the He I and He II photoelectron spectra for the 7–15-eV region of the iridium complex. This spectrum is almost superimposable with the spectrum of $(\eta^3\text{-}C_3R_3)Co(CO)_3$ in the region above 10.0 eV. The main difference is in the metal-based ionizations below 10.0 eV. An expansion of the region below 10.0 eV is shown in Figure 5. Numbers shown in the He II spectrum correspond to the change in the relative band intensity (relative to band C2) compared to the He I spectrum. Comparing this data with the spectrum of $(\eta^3\text{-}C_3R_3)Co(CO)_3$, we see that there are more bands in the Ir case and they are narrower. This trend in ionizations of third-row metal complexes has been observed previously[31] and is attributed to spin–orbit coupling due to the iridium atom (*vide infra*).

Comparing the relative intensity change of the individual bands between He I and He II, there is a decrease in intensity of bands A1 and A2 relative to band C2. Band B in the Ir complex increases in intensity relative to all the other bands in this region indicating that this has a large contribution from the metal d orbital and should be similar in orbital composition to band B of the $(\eta^3\text{-}C_3R_3)Co(CO)_3$ complex. Band C1 decreases only slightly in intensity relative to band C2. On the basis of the above trends in relative areas, we can assign bands A1 and A2 to be derived from band A of the $(\eta^3\text{-}C_3R_3)Co(CO)_3$ spectrum. Band B correlates with band B in the $(\eta^3\text{-}C_3R_3)Co(CO)_3$ case, and bands C1 and C2 are derived from C in the $(\eta^3\text{-}C_3R_3)Co(CO)_3$ spectrum. Spin–orbit coupling in the Ir case causes the resolution of five separate ionizations by lifting the degeneracy of the e ion states. All the ionizations in the Ir system are at higher binding energies than the corresponding ones in the Co system.

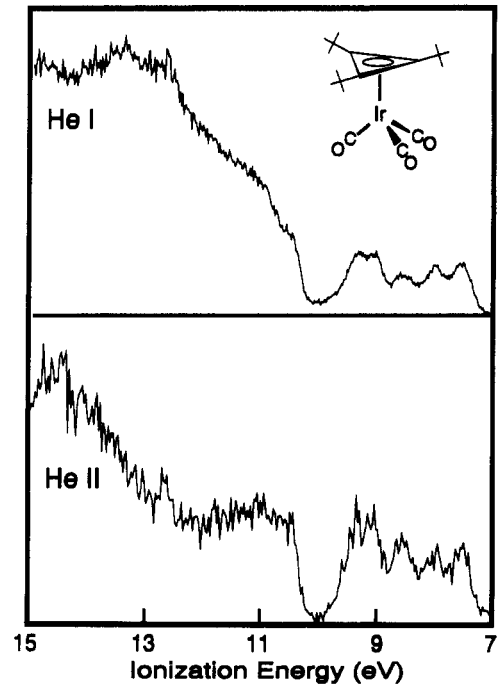

Figure 4. He I and He II photoelectron spectra of $(\eta^3\text{-}C_3R_3)Ir(CO)_3$ (where R = *tert*-butyl).

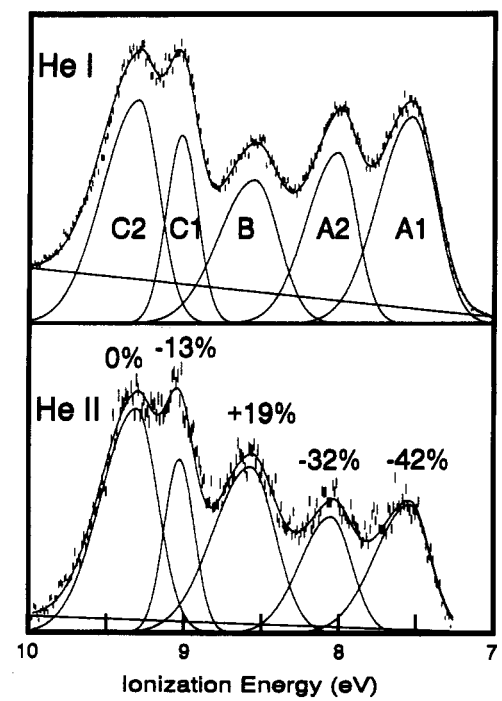

Figure 5. He I and He II photoelectron spectra of $(\eta^3\text{-}C_3R_3)Ir(CO)_3$ (where R = *tert*-butyl) in the region 10.0–7.0 eV. Numbers shown in the He II spectrum correspond to the change in the relative band intensity (relative to band C2) compared to the He I spectrum.

(31) Hall, M. B. *J. Am. Chem. Soc.* **1975**, *97*, 2057.

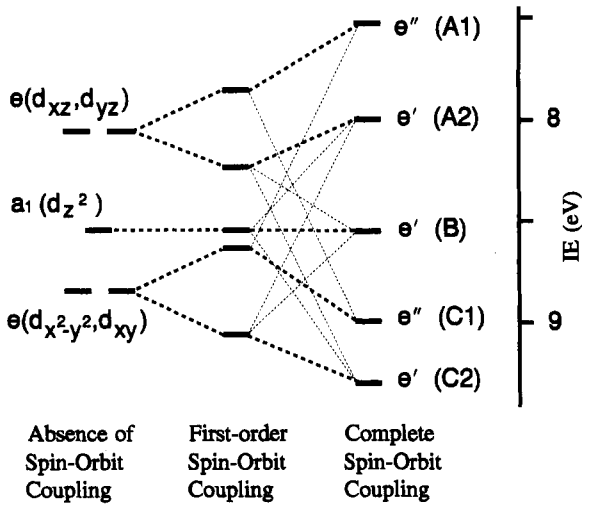

Figure 6. Approximate correlation diagram for spin–orbit coupling in the ionizations of $(\eta^3\text{-}C_3R_3)Ir(CO)_3$ (right column) based on the experimental ionization energies of $(\eta^3\text{-}C_3R_3)Co(CO)_3$ (left column, shifted 0.7 eV). The middle column represents the first-order spin–orbit splitting of the degenerate levels estimated from the atomic spin–orbit splitting pattern of iridium. Spin–orbitals of the same symmetry further interact resulting in the final level ordering shown on the extreme right.

Further support of this assignment can be obtained from the spin–orbit splittings between the bands in the Ir case. For the system of interest here, we must consider the C_{3v}* double group. Under spin–orbit coupling, the irreducible representations of C_{3v} become either e′ or e″, namely, doubly degenerate due to electron spin as follows

$$C_{3v}: \quad a_1 \quad a_2 \quad e$$

$$C_{3v}^*: \quad e' \quad e' \quad e' + e''$$

There can be coupling between e′(e) with e′(a_1 and a_2). Thus, the ionization at 7.36 eV (A) in the Co case (due to d_{xz}, d_{yz}) results in two ionizations at 7.53 and 8.01 eV (A1, A2) in the Ir case. The peak at 7.85 eV (B) in the Co complex having mainly d_{z^2} orbital character shifts to higher energy at 8.55 eV (B) in the Ir complex. Band C of the Co complex at 8.15 eV due to $d_{x^2-y^2}$ and d_{xy} ionizations gives rise to peaks at 9.02 and 9.30 eV (C1, C2) in the Ir complex. Figure 6 shows a correlation diagram based on experimental ionization energies in the Co complex. The probable range of spin–orbit coupling for Ir is 0.35–0.45 eV based on extrapolated values given by Griffith.[32] Figure 6 shows a qualitative splitting pattern due to spin–orbit coupling, assuming $\zeta = 0.4$ eV and based on the separations between peak positions in the Co case in the absence of spin–orbit coupling to be 0.47 and 0.33 eV. In the presence of spin–orbit coupling, each of the e levels splits into e′ and e″ levels. There is interaction between levels of the same symmetry leading to the levels moving up or down. This interaction results in a large energy gap between the second and third levels and a smaller energy gap between the third, fourth, and fifth levels. This splitting pattern is similar to that in the spectrum of the Ir complex. From the peak positions listed for the Ir complex in Table I, the splitting between the second and third band is 0.54 eV while that between the fourth and fifth bands is 0.28 eV.

(32) Griffith, J. S. *The Theory of Transition Metal Ions*; Cambridge University Press: London, 1961.

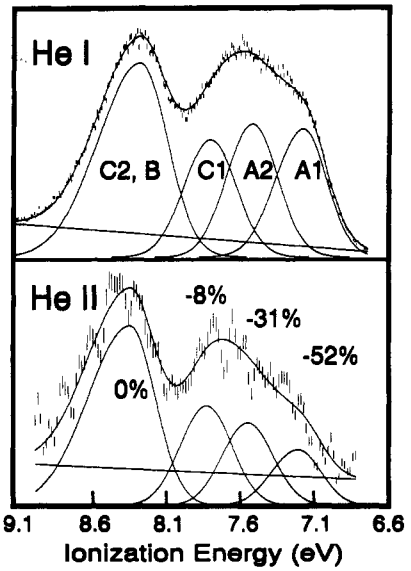

Figure 7. He I and He II photoelectron spectra of $(\eta^3\text{-}C_3R_3)Fe(CO)_2(NO)$ (where R = *tert*-butyl) in the region 9.1–6.6 eV. Numbers shown in the He II spectrum correspond to the change in the relative band intensity (relative to band C2, B) compared with the He I spectrum.

The assignment for the Ir complex is as follows: the first band e″(e) and the second e′(e) arise from e(d_{xz},d_{yz}), the third e′(a_1) has contributions mainly from d_{z^2}, the fourth e″(e) and the fifth bands e′(e) are derived from e($d_{x^2-y^2}$, d_{xy}). The relative intensity changes of the bands in the He I and He II spectra support this assignment.

$(\eta^3\text{-}C_3R_3)Fe(CO)_2(NO)$. Figure 7 shows He I and He II photoelectron spectra for the iron–nitrosyl complex in the 6.6–9.1-eV region. Numbers shown in the He II spectrum correspond to the change in the relative band intensity (relative to band C2, B) compared to the He I spectrum. The peak parameters are summarized in Table I. Considering the isoelectronic and isostructural nature of the $(\eta^3\text{-}C_3R_3)Co(CO)_3$ and $(\eta^3\text{-}C_3R_3)Fe(CO)_2(NO)$ complexes, the general similarities of the ionization features of the two complexes is not surprising. However, the stronger π accepting power of the NO ligand (compared to CO) brings about a relative stabilization of the d orbitals which are suitably oriented to donate to the NO π^* levels. Replacing CO by NO reduces the symmetry to C_s which results in splitting of the two e levels into four nondegenerate levels. The two highest binding energy levels (C2, B) are not sufficiently separated in the Fe complex and are fit with a single Gaussian peak. A minimum of three asymmetric Gaussian peaks (A1, A2, C1), is required to obtain a reasonable representation of the band between 6.6 and 8.1 eV. Unlike the case of $(\eta^3\text{-}C_3R_3)Co(CO)_3$, the relative intensity for all the peaks decreases when the source is changed from He I to He II even though the photoionization cross-sections for Fe and Co are very similar.[29] Figure 8 shows a correlation diagram between the levels of $(\eta^3\text{-}C_3R_3)Co(CO)_3$ and $(\eta^3\text{-}C_3R_3)Fe(CO)_2(NO)$. Since NO is a better π-acceptor, the metal orbitals which can back-bond to NO are stabilized. Thus, band B having a major contribution from the metal d_{z^2} orbital is stabilized, and since the high energy band could not be resolved, no intensity increase of band B can be seen.

Discussion

A starting point for the description of these compounds is in terms of a formal d^{10} metal center with the cyclo-

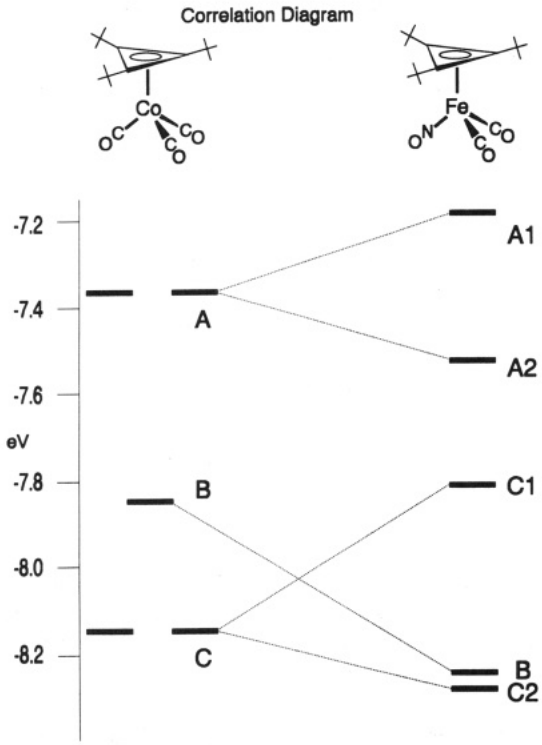

Figure 8. Correlation diagram between $(\eta^3\text{-}C_3R_3)Co(CO)_3$ and $(\eta^3\text{-}C_3R_3)Fe(CO)_2(NO)$ based on photoelectron spectroscopic data (where R = *tert*-butyl).

Table II. Comparison of the Onset Ionization Energy of the Cobalt Series

complex	approx onset of the HOMO (eV)	ref
$Co_4(CO)_{12}$	7.5	13
$(CCH_3)Co_3(CO)_9$	7.7	12
$(C_2H_2)Co_2(CO)_6$	7.8	11
$(\eta^3\text{-}C_3R_3)Co(CO_3)^a$	7.0	this work

[a] R = *tert*-butyl.

propenyl ring acting as an η^3 π system which occupies one tetrahedral coordination site of the central metal. The evidence in support of this is exhibited in several different ways. The method of synthesis involves the addition of the cyclopropenyl cation to a solution of the metal carbonyl anion. Thus, the precomplex fragments start from a formal d^{10} metal system and a unipositive cyclopropenyl ring.[7] Secondly, the angle between the carbonyls is very close to a perfect tetrahedral angle of 109° as is expected for a typical d^{10} complex. The ^{13}C NMR of $(\eta^3\text{-}C_3R_3)Fe(CO)_2(NO)$[7] shows only a single resonance for the three cyclopropenyl ring carbons, demonstrating that the cyclopropenyl ring is fluxional in nature and rotation about the cyclopropenyl–metal bond is fast on the NMR time scale even at −80 °C.

Further support of the title complexes being d^{10} tetrahedral systems is obtained from comparisons with other metallatetrahedranes. Table II compares the He I ionization onset values for the lowest ionization energy bands of the Co complex **I** (compound **3**) with those of the cobalt metallatetrahedrane series **4**, **5**, and **6**.[33] A definite and substantial break is present in the observed trend of increasing ionization energy of the HOMO as the number of Co atoms decreases. Part of the reason for the lower first ionization energy of the cyclopropenyl complex in this series is the presence of the *tert*-butyl groups in place of H or CH_3 groups. The shifts of metal-based ionizations due to H, CH_3, and *tert*-butyl substitutions on π-bound organic groups can be estimated fairly accurately because of our previous experience with methyl-substituted cyclopentadienyl complexes and because of studies by others of H, CH_3, and *tert*-butyl substitutions.[28] The shift of metal-based ionizations with three CH_3-for-H substitutions is about 0.3 eV.[34] The shift with *tert*-butyl-for-CH_3 substitution is negligible, as is the shift of the first ionization from toluene to *tert*-butylbenzene (<0.04 eV).[35] Thus, the shifts of the metal-based ionizations due to different alkyl groups are no more than a few tenths of an electron volt. The lower first IP of the cyclopropenyl complex in relation to the clusters remains significant. This trend, along with the intensity and shape of the d orbital valence band, is more consistent with Co in **I** described as a d^{10} tetrahedral system instead of the octahedral system by which other Co metallatetrahedranes have been described. Though the formal description of these cyclopropenyl complexes is in terms of a d^{10} configuration, there is substantial delocalization of electron density between the cyclopropenyl ring and the metal center. This is reflected in all three complexes by a loss in intensity in the He II spectra of the low ionization energy band (HOMO) relative to the high ionization energy band. This indicates strong interactions between the metal and the cyclopropenyl ring, and these orbitals are primarily effecting the bonding of the ring to the metal carbonyl fragment.

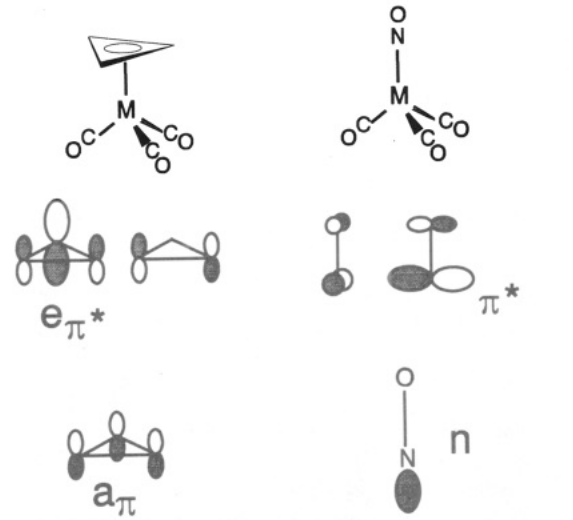

Figure 9. Orbitals of cyclopropenyl fragment and nitrosyl fragment involved in π-bonding to the $M(CO)_3$ fragment.

Comparing **I** and **III** to the isolobal nitrosyl complexes $Co(CO)_3(NO)$ and $Fe(CO)_2(NO)_2$, the σ and π^* orbitals of the nitrosyl ligand are analogous to a_π and e_{π^*} of the cyclopropenyl ring as shown in Figure 9. Figure 10 is a correlation diagram between $Co(CO)_3(NO)$ and $Fe(CO)_2(NO)_2$ based on photoelectron spectroscopic data.[16] The metal d orbitals of the cyclopropenyl complexes are destabilized by approximately 1.5 eV compared to the nitrosyl complexes. Metal orbitals that are back-bonding to the cyclopropenyl ligand lie lower in ionization energy than those primarily back-bonding to the CO ligands. However, in the nitrosyl complexes, the orbitals back-

(33) Schneider, M.; Weiss, E. *J. Organomet. Chem.* **1976**, *121*, 345.

(34) Darsey, G. P. *Diss. Abstr. Intl. B* **1988**, *49*(9), 3750.

(35) Turner, D. W.; Baker, C.; Baker, A. D.; Brundle, C. R. *Molecular Photoelectron Spectroscopy*; Wiley-Interscience: London, 1970.

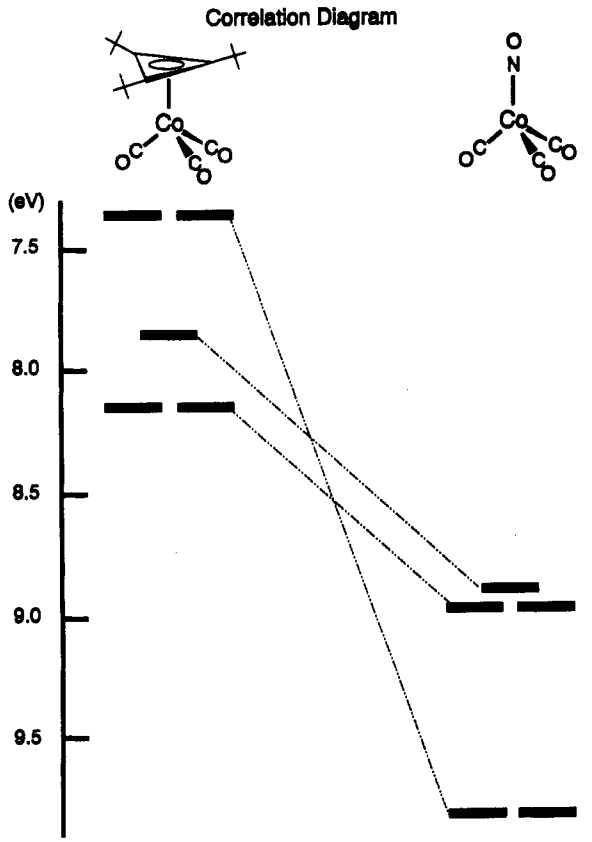

Figure 10. Correlation diagram between $(\eta^3\text{-}C_3R_3)Co(CO)_3$ (R = *tert*-butyl) and $(NO)Co(CO)_3$ based on photoelectron spectroscopic data.

bonding to the NO ligand lie higher in ionization energy than those back-bonding to CO ligands. This indicates that the nitrosyl ligand is a much better acceptor of electron density from the metal than the cyclopropenyl ring. The gap between the metal d electrons and the primarily ligand band ionizations in the cyclopropenyl complexes is significantly reduced relative to that seen in the nitrosyl compounds. This indicates that the additional ionization bands in the region 10.0–11.0 eV (in Figure 1) are due to ionizations from the cyclopropenyl rings. The highest occupied orbitals on the ring are the e_σ and a_π set and are accordingly assigned to this region.

Conclusions

Photoelectron spectra support the formal description of these η^3-cyclopropenyl metal complexes as d^{10} metals with ligands arranged in a tetrahedral array. The HOMO contains a large contribution from the e_{π^*} orbital of the cyclopropenyl ligand interacting with the appropriate d orbitals on the metal center. The orbital degeneracy seen in $(\eta^3\text{-}C_3R_3)Co(CO)_3$ is lifted in $(\eta^3\text{-}C_3R_3)Ir(CO)_3$ due to large spin–orbit coupling in the Ir atom. The HOMO in $(\eta^3\text{-}C_3R_3)Fe(CO)_2(NO)$ is similar to that in the Co complex. The metal d orbital that is back-bonding to the nitrosyl ligand shifts to higher binding energy because NO is a better π acceptor than CO.

Acknowledgment. D.L.L. and L.S. acknowledge support by the Department of Energy (Division of Chemical Sciences, Office of Basic Energy Sciences, Office of Energy Research; Contract No. DE-FG02-86ER13501) for the study of the electronic structure of organometallic molecules, the National Science Foundation (CHE-8918959) for assistance in support of the instrumentation, and the Materials Characterization Program (Arizona). R.P.H. acknowledges the support by the National Science Foundation (CHE-8907397) and thanks Johnson Matthey Aesar/Alfa for a generous loan of iridium salts.

OM920595+